Spring 5-9-2010

Changes in miRNA Expression in a Model of Microcephaly

Shan Parikh
University of Connecticut - Storrs, shansp89@gmail.com

Changes in miRNA expression in a model of Microcephaly

Shan Parikh

Physiology and Neurobiology

Abstract

miRNAs function to regulate gene expression through post-transcriptional mechanisms to potentially regulate multiple aspects of physiology and development. Whole transcriptome analysis has been conducted on the citron kinase mutant rat, a mutant that shows decreases in brain growth and development. The resulting differences in RNA between mutant and wild-type controls can be used to identify genetic pathways that may be regulated differentially in normal compared to abnormal neurogenesis. The goal of this thesis was to verify, with quantitative reverse transcriptase polymerase chain reaction (qRT-PCR), changes in miRNA expression in Cit-k mutants and wild types. In addition to confirming miRNA expression changes, bio-informatics software TargetScan 5.1 was used to identify potential mRNA targets of the differentially expressed miRNAs. The miRNAs that were confirmed to change include: rno-miR-466c, mmu-miR-493, mmu-miR-297a, hsa-miR-765, and hsa-miR-1270. The TargetScan analysis revealed 347 potential targets which have known roles in development. A subset of these potential targets include genes involved in the Wnt signaling pathway which is known to be an important regulator of stem cell development.

Introduction

Neocortical development during embryogenesis depends on proper functioning of the stem cell population in the ventricular zone (Li et al. 2010). Neural stem cells exhibit two critical properties: self-renewal and multipotency. Factors that contribute to the regulatory pathways that maintain these properties are significant for future clinical applications that may compensate for cases of disrupted neurogenesis. MiRNAs have been implicated in regulating the properties that constitute a stem cell. As an example, antagonisms between specific miRNAs and the TRIM32-let7 pathway determine the balance between stem cell differentiation and proliferation (Li et al 2010). Evidence that links miRNAs to neurogenesis is mounting and has demonstrated that miRNAs are involved in processes varying from stem cell self-renewal, fate determination, to neuronal maturation (Cuif 2009).

Citron kinase is a gene that is crucial for regulating cytokinesis during neocortical development. Mutants with a single base pair deletion, in exon 1 of the gene that codes for Citron kinase (cit-k), result in the formation of an early stop codon and an associated nonfunctional protein. (Sarkasian 2002). Such mutants are referred to as flatheads (*fh*), which are characterized by a microcephaly phenotype resulting from improper neuronal replication. These defects are mainly attributed to the loss of cit-k expression among neuronal progenitors in the ventricular surface resulting from a failure in cytokinesis. It is suggested by Sarkisian (2002) that the bi-nucleation that develops due to the impairment in cytokinesis results in genomic instability and accompanying apoptosis. Although the major defects that arise from the cit-k mutation are known, transcriptome analysis reveals a broad accompaniment in downstream changes that

signifies interaction with other genes. The miRNAs that are regulated may provide insight into understanding the phenotypic differences that accompany the cit-k mutation.

miRNAs are small, 18-24 nucleotide long, non-coding RNAs, that function in the post-transcriptional regulation of gene expression (Cuif 2009). Their mechanism of inhibition involves partial complementary base pairing with the 3' un-translated region of target mRNAs (Wu 2008). According to Wu (2008), depending of the degree of complementarity, the miRNA can act to partially suppress translation of the mRNA, or can completely degrade it. While attempting to uncover miRNA function it is important to consider the broad range of mechanisms by which miRNAs have been proposed to modulate gene expression. Depending on the protein to miRNA interaction, varying methods of repression have been proposed. The complex that mediates transcript alteration is termed the RNA-induced silencing complex (RISC), which functions to match the miRNAs to complementary sites on the target transcript. The core protein that comprises this complex includes isoforms of Argonaute (Ago) and result in variant dependent alterations to the transcript. For example, RISCs associated with Ago2 functions as endonucleases to excise regions of the mRNA that are fully complementary to the miRNA (Wu 2008). Other Ago proteins, including Ago1- Ago4, act by suppressing translation and accelerating de-adenylation in hopes of destabilizing the mRNA into degradation (Wu 2008). In addition to excision of the mRNA and de-adenylation, separate mechanisms have been proposed that function by competing at the 5' cap with the eIF4E initiation factor (Wu 2008). Although the initial step requires partial complementary binding of the miRNA to a region on the mRNA, it is clear that multiple mechanisms are enacted by this process to facilitate the suppression of mRNA translation. Uncovering the mechanism by which the regulated miRNAs suppress translation may provide input on their relationship to neurogenesis.

The goal of this thesis was to verify the RNA-sequencing data through qRT-PCR. The RNA analyzed was identical to that used for deep sequencing. Samples were isolated from both flathead and wild-type rat brain and cultured cells. The isolated RNA served as a template for cDNA synthesis. Primers for qRT-PCR were designed from the pre-pri-miRNA sequences from the miRNAs of interest. Completion of qRT-PCR confirmed differences in miRNA expression between the flathead and wild-type tissue samples based on amplification of the selected primers. The resulting data was analyzed and compared to the previously conducted RNA deep sequencing. The miRNAs that were confirmed to change include: rno-miR-466c, mmu-miR-493, mmu-miR-297a, hsa-miR-765, and hsa-miR-1270. Alongside the confirmed regulation, bioinformatics analysis was conducted in hopes of revealing potential downstream targets of the regulated miRNAs. TargetScan 5.1 predicts potential targets of miRNAs based on the homology of sequence between the miRNA and the target mRNA. Although 347 targets were predicted, comparison with the deep sequencing data revealed only 46 genes that varied significantly (>1.5 or <-1.5).

Materials and Methods

RNA Isolation

RNA was isolated from an n = 3 of flathead and wild-type forebrain and n = 3 flathead and wild-type progenitor culture, using the Ambion RNAqueous kit. Tissue was acquired from embryonic day 13 specimen or equivalent. For tissue preparation, tissue was homogenized with the addition of 500 µL of 10 µg/mL Lysis/Binding solution. Sonication of tissue was then completed for further homogenization of tissue followed by centrifugation for 2-3 minutes at 16000xg for purification. Subsequently, 500 µL of 64% Ethanol was pipetted into each lysate and vacuum filtered through a filter cartilage. Lysates were centrifuged and any flow-through

was discarded. Filter cartridges were then washed with 700 µl of Wash Solution #1 and two 500 µl aliquots of Wash Solution #2/3. Flow-through was discarded after each wash, and the resulting samples were centrifuged for 3 minutes in order to remove any excess wash solution. After transferring to a fresh collection tube, bound RNA was eluted twice using preheated (80º C) Elution Solution. A 30-second centrifugation after each aliquot was performed to collect the eluate. RNA concentrations were measured for each sample through the use of a Nanodrop© spectrophotometer at 260 nanometers. Isolated RNA was stored at -20º C.

cDNA Synthesis

cDNA synthesis was conducted using Invitrogen SuperScript III. Briefly, 1 µg of isolated RNA from each sample (n = 3 tissue RNA or n = 3 progenitor culture RNA) was pipetted into a tube containing 1 µl 50 µM oligo$(dT)_{20}$ primer. Another 1 µl of 10 mM dNTP mix was added, and the total volume was brought up to 10 µl using DEPC-treated water. After 5 minutes of incubation at 65º C and 1 minute on ice, 10 µl cDNA Synthesis Mix was added to each tube. Synthesis Mix contained 2 µl 10X RT buffer, 4 µl 25 mM $MgCl_2$, 2 µl 0.1M DTT, 1 µl RNaseOUT and 1 µl SuperScript III RT. Following centrifugation, the mixtures were incubated for 50 minutes at 50º C, and then for 5 minutes at 85º C to terminate the reaction. Samples were centrifuged and 1 µl RNase H was pipetted into each tube to remove any RNA. After a final incubation of 20 minutes at 37º C, synthesized cDNA was stored at -20º C.

Primer Design for miRNAs

Primers required for qRT-PCR completion were designed using the Primer3 software (http://frodo.wi.mit.edu/primer3). Coding sequences used for primer design were selected for from the miRNBase (http://www.mirbase.org). Specifically, nucleotide sequences from the pre-pri-miRNA were used (Table 1). Insertion of the coding sequence for the selected miRNAs into

the Primer3 software resulted in functional primers (Table 2). Primers were designed with specific parameters for proper function. The product size range was restricted to between 105 and 175 base pairs for optimal qRT-PCR amplification. Primer GC percentage was kept within a range of 20 to 80 and a GC clamp was added to promote stronger binding affinity. Primer T_m was optimized at 65º C; with a 60º C to 70º C range, and primer size was limited to 18-22 base pairs. Resulting primers from Primer3 were assessed for specificity using NCBI Blast (http://blast.ncbi.nlm.nih.gov/Blast.cgi). Only primers with low E values were selected for primer creation.

MiRNA	**Pre-pri-miRNA sequence**
rno-miR-466c	CCUGUGUGUAUGUGAUGUGUGCAU GUACAUGUGUGUAUAUGGAGAAAC AUAUACAUGCACACAUACACACACA CAGGCA
mmu-miR-493	CGCCAGGGCCUUGUACAUGGUAGGC UUUCAUUCAUUUUUUGCACAUUCGG UGAAGGUCCUACUGUGUGCCAGGCC CUGUGCCA
mmu-miR-297a	AUAUGUAUGUAUGUAUGUAUGUGU GCAUGUGCAUGUGCAUGUAUGCAUA UUGCAUGUAUAUAUUAUGCAUACA UGU
hsa-miR-765	UUUAGGCGCUGAUGAAAGUGGAGU UCAGUAGACAGCCCUUUUCAAGCCC UACGAGAAACUGGGGUUUCUGGAG GAGAAGGAAGGUGAUGAAGGAUCU GUUCUCGUGAGCCUGAA

hsa-miR-1270	CACAGAGUUAUACUGGAGAUAUGG AAGAGCUGUGUUGGGUAUAAGUAA CAGGCUUUUCUUUAUCUUCUAUGUG GCUCUUUGCA

Table 1: Pre-pri MiRNA coding sequence

MiRNA	Left Primer	Right Primer
rno-miR-466c	tcagaaccggcctctcatcc	acctcggcgtcagcttcatc
mmu-miR-493	cagatgccttgcggttcctc	cattgatgtccgccaggttg
mmu-miR-297a	caagaatggaagcagcgaagg	ctctggagccagccagtgtg
hsa-miR-765	cggtgaacaagcgagagtcg	aatagtcgcgcggcttctgg
hsa-miR-1270	cttgtgctcgccactgttgg	aatagtcgcgcggcttctgg

Table 2: Primer sequences from Primer3

Quantitative RT-PCR

Upon synthesis of cDNA using reverse transcriptase, qRT-PCR can be completed to measure amplification. QRT-PCR was performed using the Applied Biosystems ABI 7500 Fast Real Time PCR System. Plates were prepared with reaction volumes of 20 μL per well including the following: 9 μL primer mix, 1 μL cDNA, and 10 μL SYBR Green. Plates were run in the PCR machine at 40 cycles with the following parameters: 94º C for 2 s, 60º C for 30 s and 72º C for 30 s. Amplification levels are determined by comparison to the gene Gapdh; a housekeeper gene that is expressed in all cells independent of Cit-k expression. Detection of amplification is dependent on measurement of the increase in fluorescence as the SYBR Green binds to the amplified amount of double stranded DNA in the reaction tube. The quantification mechanism applied is known as Delta Delta CT, which is an approximation method that corrects for baseline expression of the standard gene, Gapdh in this case.

TargetScan 5.1 Analysis

Potential downstream targets of the regulated miRNAs were found through TargetScan 5.1. Insertion of miRNA names into the database with specification of conserved targets resulted in a list of all possible genes with complementation of the miRNA seed sequence to the 3' un-translated region of the gene. Once a list was generated, regulation levels from the RNA sequencing data was tabulated for each predicted target.

Results

RNA Isolation

Table 4 is a list of all RNA concentrations from the Nanodrop© from both forebrain and cultured cells.

Forebrain Tissue	**ng/µL**		**Neural Progenitor Tissue**	**ng/µL**
WT 1	890.86		WT 1	522.46
WT2	723.27		WT2	239.9
WT3	860.06		WT3	452.98
*FH*1	800.83		*FH*1	833.94
*FH*2	681.89		*FH*2	830.19
*FH*3	607.85		*FH*3	478.2

Table 4: RNA concentrations

qRT-PCR

PCR data for both forebrain and cultured cells verifies up-regulation of all selected miRNAs. Similar levels of regulation between PCR and RNA sequencing provides convincing evidence for increased levels of these miRNAs. miRNA 466c showed similar values of up regulation with a 4.2 fold regulation in RNA sequencing, 3.2 fold in qRT-PCR of forebrain tissue, and a 4.6 fold in culture cells. miRNA 493 respectively displayed up regulation of 8.1, 6.4, and 7.4. Regulation here is also quite comparable. However, the remainder of the miRNAs

varied to a greater extent as seen in Figure 2. Although slight disparities exist, all miRNAs are within 4 fold regulation of data from the two verification techniques used.

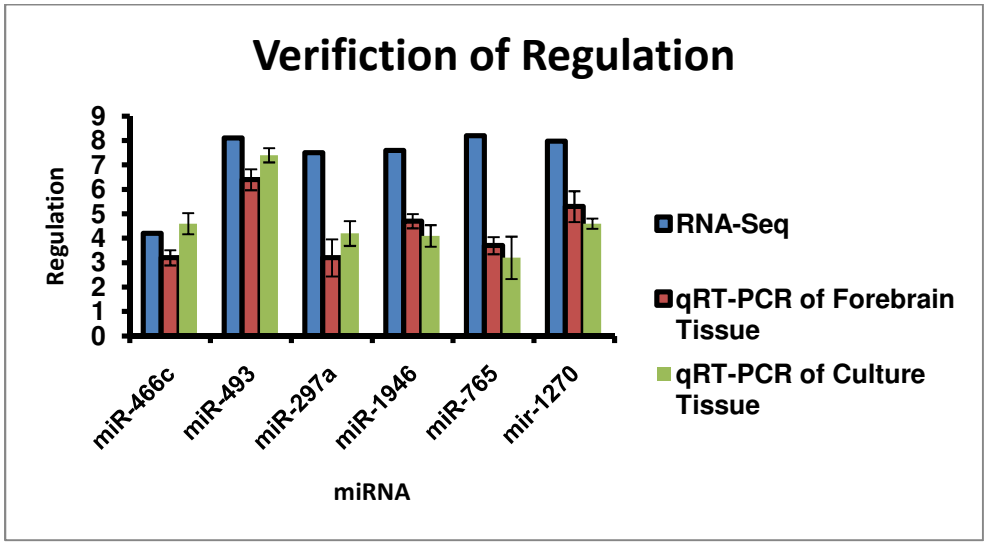

Figure 2: Comparison of qRT-PCR of forebrain and culture tissue versus RNA sequence regulation

TargetScan 5.1 Predicted Targets

Upon analysis of all predicted genes from TargetScan 5.1, we found that there were nearly 347 genes and many were regulated to a minimal degree (included in Appendix 1). To increase experimental potential, only genes that were up or down regulated by a factor of 1.5 or more are displayed and will be further investigated. Alongside the RNA sequencing data, the probability of interaction (context score) is also tabulated for systematic sorting. Table 5 displays the predicted gene targets with their associated regulation and context values.

miRNA	Predicted Gene	>1.5	Context score	Predicted Gene	<-1.5	Context score
rno-mir-466c	PBRM1	2.318	-0.45	LMX1B	-1.5	-0.12
	ZFAND5	1.88	-0.34	FSCN3	-2.25	-0.22
	NFIB	1.77	-0.14			
	TRPS1	1.69	-0.43			
	CDH11	1.63	-0.2			
	GTDC1	1.61	-0.14			
hsa-mir-1270	STC2	4.66	-0.31	BSN	-1.56	-0.27
	CTSE	2.426	-0.48	PAK6	-1.6	-0.18
	TFPI	2.402	-0.3	GRIN2D	-1.6	-0.16
	STXBP4	1.96	-0.16	CNTN3	-1.718	-0.55
	OLA1	1.769	-0.43	KIAA1024	-2.62	-0.18
	NEGR1	1.69	-0.21			
	ABCC4	1.66	-0.38			
	GTDC1	1.611	-0.49			
	TFRC	1.6	-0.17			
	CPEB2	1.53	-0.49			
	TBX15	1.53	-0.25			
mus-mir-493	RAB30	1.759	-0.14	NCOR2	-1.44	-0.15
	GRIA4	1.7086	-0.05	CPLX1	-1.49	-0.38
	SLC13A1	1.498	-0.37	CIC	-1.704	-0.37
mus-mir-297a	NRXN1	1.91	-1.05	SPEN	-1.56	-0.25
	CADM2	1.846	-0.25			
	SMOC2	1.774	-0.37			
	CUGBP2	1.697	-0.1			
	AZIN1	1.6689	-0.41			
	EIF2C3	1.628	-0.46			
	ZFX	1.57	-0.42			
	SKIV2L2	1.493	-0.32			
hsa-mir-765	STC2	4.6672	-0.08	CPLX1	-1.49	-0.43
	C1QC	2.5168	-0.31	GLIS2	-1.5	-0.36
	ZDHHC21	1.948	-0.07	FBXL19	-1.5	-0.21
	DNAJC13	1.78	-0.09	DIRAS2	-1.53	-0.27
	SPOPL	1.669	-0.42	BSN	-1.56	-0.3
	SLC18A3	1.668	-0.2	RGS16	-1.6	-0.31
	GABRA3	1.665	-0.35	MBD6	-1.68	-0.15
	ANKRD45	1.619	-0.42	PSD4	-1.69	-0.05
				KCND1	-1.76	-0.83

Table 5: Predicted gene targets and associated context scores from TargetScan 5.1

Discussion

Implications of Verification

The precision of the experimental techniques used in this thesis are demonstrated by the similarity in results. Regulation of the selected miRNAs in the *fh* are significantly increased in both the deep sequencing experiment and in the qRT-PCR experiment of both culture and forebrain cells. Verification of the regulation of these miRNAs is significant in establishing a base for further experimentation of their downstream targets. Furthermore, data from the genomic analysis of forebrain tissue presents that the intergenic reads show 100% homology to non-rat miRNAs that were analyzed in this experiment. This suggests that the miRNAs discovered in the deep sequencing data are conserved across species and involved in similar processes as a measure of clinical significance.

Experiments in culture further demonstrated the regulation of the assessed miRNAs, however in a more controlled fashion. Neural progenitor cells from wt and *fh* forebrain were cultured and their identities were confirmed by Nestin staining. Staining with Nestin affirms the presence of neural progenitor cells due to absorption by intermediate filaments typically found in neural epithelial cells and radial glia. Presence of Nestin stain confirms that the expression of the miRNAs of choice was localized to the neuronal progenitor cells and not from other cell types. This is important in studying the true impact of miRNAs on the regulatory loops of these progenitors.

TargetScan 5.1

TargetScan 5.1 was utilized for predicting potential downstream targets of the miRNAs of interest. This bioinformatics software operates by matching the seed sequence (position 2-8) of the mature miRNA to complementary regions on the potential mRNA. Although such analysis

does not provide guaranteed interactions, there is a degree of specificity based on the context score. Context score is calculated based upon several factors with the lowest or most negative score being the most favorable prediction. According to Grimson et al (2007), the five general features that contribute to increasing the probability of interaction within this software are as follows:

1. AU-rich nucleotide concentration near the site of interaction
2. Proximity to sites for co-expressed miRNAs
3. Proximity to residues paired to miRNA nucleotides 13-16
4. Positioning within the 3' UTR at least 15 nucleotides from the stop codon
5. Positioning away from the center of long UTRs.

Several of the sorted predicted targets are listed with their corresponding context scores in Table 5. Use of this probability measure will serve as guide for future experimental design. Also, multiple programs for target prediction exist. For increased accuracy in the prediction of targets, a comparison of results can be completed with other software.

Pathway Analysis

Genetic pathway analysis programs (Panther and DAVID) were utilized for screening purposes. These programs allow for the input of large numbers of genes for comparison with substantiated genetic pathways that are specified in data banks. The resulting output consists of the cataloging of the genes into known biological pathways. The list of miRNA targets generated from the TargetScan analysis was analyzed with these programs resulting in the prediction of three main pathways: regulation of axon cytoskeleton, axon guidance, and Wnt (Appendix 2a,b,c). Since very few single miRNA gene mutations result in a noticeable phenotype and since most genes are targets of multiple miRNAs, it appears that interactions between multiple

miRNAs and their targets genes result in biological changes (Inui et al 2010). For this reason systematic screening of these genes targets is further potentiated in accurately making predictions of the functions of these miRNAs.

Data from Panther shows: DAAM2, LRP6, PPP2R5c, TBL1X, and TBL1XR1 to be involved in Wnt signaling. All of which are predicted gene targets of the regulated miRNAs. The Wnt signaling cascade is comprised of a network of proteins critical to embryonic development as well as normal physiology. Also, recent evidence has implicated the Wnt pathway in stem cell renewal (Inui et al 2010). In stem cells, Nanog (a transcription factor) has been shown to be a critical factor for the maintenance of the self-renewal; a signature property of stem cells. Wnt signaling often leads to the downstream activation of TCF in response to the accumulation of β-Catenin in the nucleus (Inui et al 2010). TCF subsequently acts as a competitor for co-repressors that associate with target genes, in this case Nanog (Pereira et al 2006). Due to the effects of the cit-k mutation on the neural progenitor population where stem cell proliferation is rampant, implication of the Wnt cascade by pathway mapping programs is even more feasible.

Future Experiments

Although data gained was plentiful, I believe it is insufficient for proper pathway mapping. Only 5 of the 34 miRNAs that are regulated in the *fh* were confirmed and matched with possible targets. In order to thoroughly analyze the data and gain true perspective on possible genetic pathways, it is essential that all miRNAs are verified and analyzed. Pathways mapping programs such as Panther and DAVID aid in analysis, and larger inputs of genes into these programs will result in more accurate predictions of the impact of miRNAs on these pathways. Essentially, verification of all miRNAs and target analysis must be completed for further

experimentation. If, and once, pathways are predicted, animal models can be utilized to further study the impacts of miRNAs on the pathways of interest.

References

Cuif, L. & Coolen, M. (2009). MicroRNAs in brain development and physiology. *Current Opinion in Neurobiology,* 19, 1-10.

Dennis G Jr, Sherman BT, Hosack DA, Yang J, Gao W, Lane HC, Lempicki RA. DAVID: Database for Annotation, Visualization, and Integrated Discovery. *Genome Biol. 2003;4(5):P3.*

Inui, M. & Piccolo, S. (2010). MicroRNA control of signal transduction. *Nature Reviews*, *11*, 252-263.

Grimson A, Bartel DP et al (2007). MicroRNA Targeting Specificity in Mammals: Determinants beyond Seed Pairing. *Molecular Cell*, 27 (1), 91-105.

Gutman GA, Chandy KG, Grissmer S, *et al.* (2006). "International Union of Pharmacology. LIII. Nomenclature and molecular relationships of voltage-gated potassium channels."*Pharmacol. Rev.* **57** (4): 473–508.

Pereira L, Yi F, Merrill BJ (October 2006). "Repression of Nanog gene transcription by Tcf3 limits embryonic stem cell self-renewal". *Mol. Cell. Biol.* **26** (20): 7479–91.

Sarkisian, Matthew R. et al. (2002). Citron Kinase, a Protein Essential to Cytokinesis in Neuronal Progenitors, is Deleted in the *Flathead* Mutant Rat. *The Journal of Neuroscience*, 22 : RC217, 1-5.

Thomas, P. & Narechania, A. (2003). PANTHER: A Library of Protein Families and Subfamilies Indexed by Function. *Genome Research*, *13*, 2129-2141.

Rozen S, Skaletsky H. (2000) Primer3 on the WWW for general users and for biologist programmers. In: Krawetz S, Misener S (eds) *Bioinformatics Methods and Protocols: Methods in Molecular Biology.* Humana Press, Totowa, NJ, pp 365-386.

Wu L, Belasco J. (2008) Let Me Count the Ways: Mechanisms of Gene Regulation by miRNAs and siRNAs. *Molecular Cell,* 29, 1-7.

Appendix

1) All Predicted Gene Targets

miRNA	rno-mir-466c	hsa-mir-1270	mus-mir-493	mus-mir-297a	hsa-mir-765
Predicted Gene Targets	PBRM1 ZFAND5 NFIB TRPS1 CDH11 GTDC1 CUC2 CLPT UBE2N ASH1L UBE2K ZDHHC3 HHIP DAZAP2 DCX EYA1 KPNA1 SLC39A14 APIS SERF2 DRD2 KLF12 ANKH SMEK1 KIAAO314 TBL1XR1 PAFAH1B1 H3F3B STX16 ANKRD11 CNOT2 GABBR2 HLF	STC2 CTSE TFPI STXBP4 FAM152A OLA1 NEGR1 ABCC4 GTDC1 TFRC CPEB2 TBX15 UBE2G1 KIT1G TGM2 TNRC6B PCYOX1 MED17 L2HGDH GOLGA3 LRRCC1 DCX FAM8A1 ITCH MARCH.5 HNRNPC COP52 ALPH1A SORBS1 MMP16 MGA TC2N LRP4	RAB30 GRIA4 SLC13A1 EEF1A1 PURB PDE4D RND2 KIF3B COL5A1 B4GALT6 PRKAA2 CAPN6 KPNA1 PPP2R1B ST8SIA3 SEMA4F HDLBP ANKRD17 PSMD7 N4BP1 AAK1 TBC1D20 ADAM17 ZBTB34 FOXP2 PLXNA2 NFASC SH3PXD2A ZNF618 TMEM35	NRXN1 CADM2 SMOC2 CUGBP2 AZIN1 EIF2C3 ZFX SKIV2L2 WSB1 SMC6 SNX13 ATRN TNRC6B WHSC1 ARHGAP28 PCSK2 SLC1A2 PIK3AP1 FBXW2 CPSF2 ORMDL2 SETD8 DNAJC21 PPP2R5C COPS2 ARHGEF12 KIAA1853	STC2 C1QC ZDHHC21 DNAJC13 SPOPL SLC18A3 GABRA3 ANKRD45 CD34 TMED10 FXR1 TCF4 TLK2 RPL13A RAB6A GPC3 PTPRT SLC11A1 MEIS1 NXN PURB IVNS1ABP MAML3 ARL2 NUTF2 SLC2A4 CACNA1E LMNA SNX1 CAPN6

	MLF2 LMX1B FSCN3	MAPK14 KIF1B CUL4B ODZ4 WHSC1 ARHGEF4 CD248 SCAMP5 SPTBN1 SYT11 RAPH1 DAAM2 HELZ CTNS KIAA1024 FAM123B STAU1 SEMA6A EIF4B GALNT2 ARID1B CYFIP2 CHSY1 SENP5 HNRPU OTND3 RIMBP2 POU2F2 AK2 PATL1 KHDRB3 CCNT2 SLITRK2 STAT2 PIP4K2B CBX1 CHRM1 PRR3	NAV1 RIMS4 CFL1 FMR1 NCKAP1L PITPNM2 MAP2K7 NCOR2 CPLX1 CIC	ARNT CAMTA2 SNAP91 USP49 PATL1 CCNT2 WBP1 NEUROD1 AFF4 SIPA1L2 ZFP36L1 TNK1 ZBTB38 R3HDM2 BCL11B SOX12 SLC26A7 SPEN	NTRK3 FAM134C CCDC51 USP7 GATAD2B PRRX1 LRP6 TBL1X DENND1A TRMT5 GBF1 PLD4 C20orf160 CREB3L2 GCN1L1 AAK1 RNF41 DYSF MTMR4 TIMP3 NSFL1C CDK2 SCAMP5 KANK4 SLCO2B1 RAP2B CBFA2T2 DHDDS MSN SHROOM4 RUNX1T1 ARID2 WDR78 EIF2C1 YBX2

		CLSTN2 TCF20 DABZIP UNC84B PCDH10 PMC IPTK1 CAPRIN1 BZRAP RIM54 CELSR2 MARK4 MXD1 FURIN PAPRD FOXO3 BSN PAK6 GRIN2D CNTN3 KIAA1024			RANBP10 EGLN2 FOXN3 IGFBP5 KLHL18 TMEM184B CALU SLC22A17 TBC1D22B NIP30 SLC36A1 POU2F2 HEYL PSD2 DENND2C DOK2 ZNF512 PPP1R12B NDST1 CYB561D1 SFRS2 CAPN3 THRAP3 IGF2BP1 WDTC1 NFIX FXR2 PACS1 MFHAS1 NCOA5 MDGA1 TMEM158 STK4 DPYSL5 MYO1A

					ANKRD52 G3BP2 NAV1 MYD88 LPHN1 VAMP2 ATXN7L2 SEMA4G THRA AKAP5 CALM3 SPTB ST3GAL2 VASH1 MICAL3 CADM4 TNS1 ProSAPiP1 HIC2 MEX3A GPR84 LINGO1 CPLX1 GLIS2 FBXL19 DIRAS2 BSN RGS16 MBD6 PSD4 KCND1

2) DAVID Predicted Pathways

a) Regulation of actin cytoskeleton

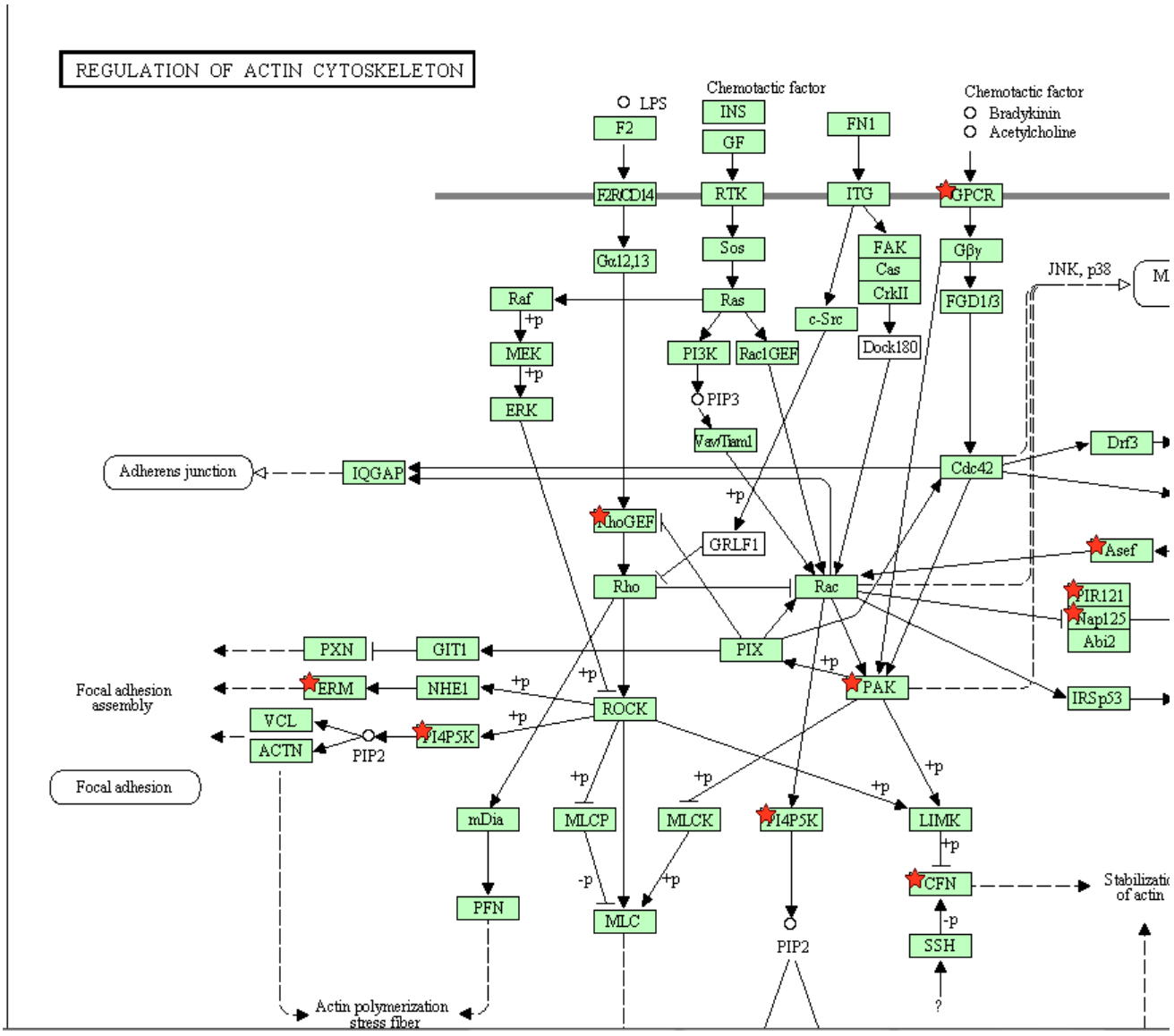

b) Axon Guidance

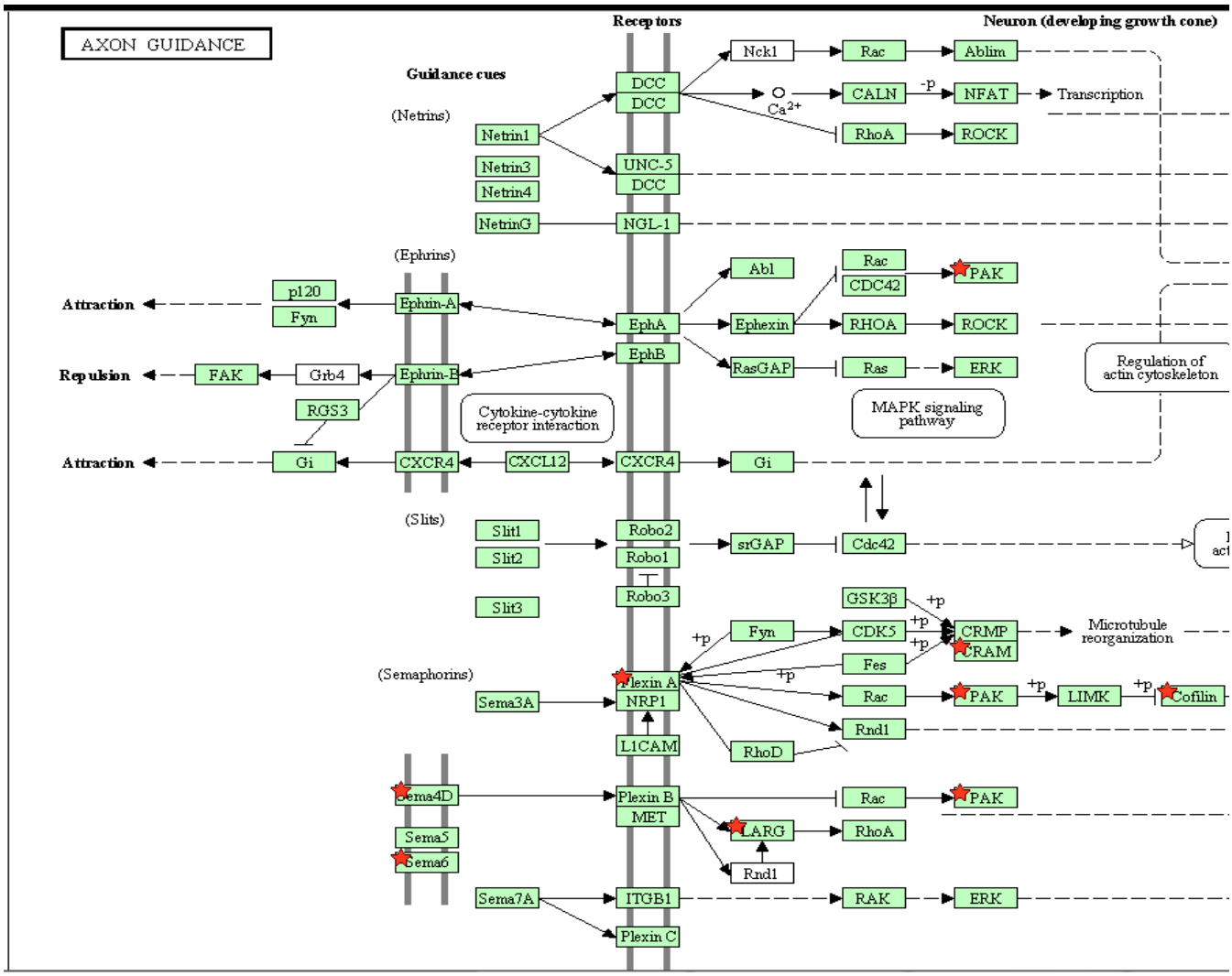

c) Wnt Pathway